MJFAS MALAYSIAN JOURNAL OF FUNDAMENTAL AND APPLIED SCIENCES
PRINT ISSN: 2289-5981 | ONLINE ISSN: 2289-599X

RESEARCH ARTICLE

Numerical modelling of blood cells distribution in flow through cerebral artery aneurysm

Syazatul Aniza Arshad [a], Osama Sabir [a], Joanne Huang [b], Kevin Ly [c], Angela Nguyen [b], Tuan Mohammad Yusoff Shah Tuan Ya [a,*], Sobri Muda [d], Adli Azam Mohammad Razi [e], Anis Suhaila Shuib [f]

[a] Mechanical Enginering Department, Universiti Teknologi PETRONAS, 32610 Tronoh, Perak, Malaysia
[b] Department of Chemical and Biomolecular Engineering, Lehigh University, Bethlehem, Pennsylvania, USA
[c] Department of Bioengineering, Lehigh University, Bethlehem, Pennsylvania, USA
[d] Deparment of Radiologi/Neuroradiologi & Neurointervensi, Universiti Putra Malaysia, 43400 UPM Serdang,Selangor Darul Ehsan
[e] Cardiovascular and Thoracic Surgery Unit, Surgical Science Cluster, Faculty of Medicine, Universiti Teknologi MARA, Sungai Buloh Campus, Jalan Hospital, 47000, Sungai Buloh, Selangor, Malaysia.
[f] Deparment of Chemical, Taylor's University Lakeside Campus, Jalan Taylors, Subang Jaya, 47500 Subang Jaya, Selangor, Malaysia

* Corresponding author: tyusoff.ty@utp.edu.my

Article history
Submitted 17 November 2017
Revised 13 February 2018
Accepted 28 February 2018
Published Online 28 Mac 2018

Abstract

Recent aneurysm studies have focused on the correlation between different parameters and rupture risk; however, there have been conflicting findings. Computational fluid dynamics (CFD) allows for better visualization but idealized aneurysm models may neglect important variables such as aneurysm shape and blood flow conditions. In this paper, one case of an aneurysm was studied with CFD using a non-Newtonian Power Law Model to investigate the correlation between wall shear stress and blood cells distribution. Results show that velocity of blood flow decreased as it entered the aneurysm and the neck of the aneurysm experienced a greater magnitude of wall shear stress than the remainder of the cerebral artery. Besides, the blood cells generally begin at low velocities and increase after the first curve of the artery. Findings and further studies with larger cases of patients will improve treatment and prevention of aneurysm ruptures.

***Keywords*:** Aneurysm, CFD, wall shear stress, blood cells

INTRODUCTION

Brain is the center of nervous system which consists billions of cells which divided into cerebrum, cerebellum and stem. Blood supply to brain is important to meet the metabolic demands. The average adults have about five liters of blood living inside of their body, coursing through their vessels. Blood function in delivering essential elements, and removing harmful wastes. Hence, without blood, the human body would stop working. Blood is a multicomponent fluid consists of 45% formed elements suspended 55% plasma liquid by volume. Formed elements consist of red blood cells (RBCs) or erythrocytes (99.9%), white blood cells (WBCs) or leukocytes and platelets where combination of these two resulting in the remaining 0.1% of formed elements.

An aneurysm is a ballooning of an artery, cerebral artery that carry blood from the heart to other parts of the body. They can occur throughout the body, including the aorta and the brain. Often times, small aneurysms go undetected and are discovered unexpectedly when other medical tests are performed. When a cerebral aneurysm bursts, symptoms include sudden headache, stiff neck, and nausea, and the subsequent intracranial hemorrhage is associated with high mortality rates (Munarriz et al., 2016).

Aneurysms develop due to the weakening of the cerebral artery wall. Research has been done to determine the correlation of different parameters to risk of aneurysm rupture. Prior studies show that factors such as larger aneurysm size, aspect ratio, and size ratio are associated with an increased risk of rupture (Jiang et al., 2014) (Dhar et al., 2008). Recently, hemodynamic factors have been of interest to predict aneurysm rupture more accurately. Larger areas of low wall shear stress (WSS), the force tangential to wall, along the dome has been associated with increased risk of rupture (Xiang et al., 2011) (Goubergrits et al., 2012). On the contrary, high wall shear stress is correlated with formation of bifurcation aneurysms and is negatively correlated with the formation of sidewall aneurysms (Can and Du., 2016).

Hemodynamic parameters will provide a better understanding of aneurysm formation, growth, and rupture, leading to improved treatment for patients with unruptured aneurysms. The pathology of aneurysm rupture involve cells and low flows of blood cells will caused localized blood-flow stagnation againts wall in the aneurysm dome. A stagnation of blood can cause a dysfunction of flow that induced Nitrogen Oxide and caused intimal damage, leading to infiltration of white blood cells and fibrin inside the aneurysm wall. This study aims to examine blood cells distribution through simulations on ANSYS Fluent for computational fluid dynamics (CFD) analysis. Previous studies with CFD analysis used idealized models and structured aneurysms. By using patient-specific aneurysm geometries, more specific results can be provided for the respective patient (Cebral, Castro, Appanaboyina, et al., 2005). Simulations are run using non-

Newtonian models to investigate the correlation of WSS to aneurysm rupture. CFD approach allows for better visualization and understanding of the hemodynamics and correlation of parameters to rupture risk.

METHODOLOGY

Aneurysm Geometry and Meshing

In order to have an appropriate model of an aneurysm, an interventional neuroradiologist specializing in aneurysms in the cerebral artery from the Hospital Universiti Kebangsaan Malaysia (HUKM) provided angiograms of four real-life cases of patients who had an aneurysm. But in this paper, only one case will be discussed which is middle cerebral artery. For each case, the angiograms were in Digital Imaging and Communications in Medicine (DICOM) format which has 256 stacks of images. The images were analyzed in order to determine what the most optimal geometry of each aneurysm would be for future simulations.

To prepare the images for simulation use in ANSYS Fluent, the images was processed in an image processing software Mimics Research 19.0. Mimics allows for segmentation of the aneurysm and surrounding cerebral arterys so that a better and more focused image of the aneurysm could be produced. For the purposes of the simulation, the inlet cerebral artery to the aneurysm was made to be significantly longer than the outlet cerebral artery. The segmented image was processed in 3-matic Research 11.0. To produce a mesh file that is compatible with ANSYS Fluent. Figure 1-4 shows the procedure from when the image was first receivedto the final mesh.

Fig. 1 Angiogram image in DICOM format.

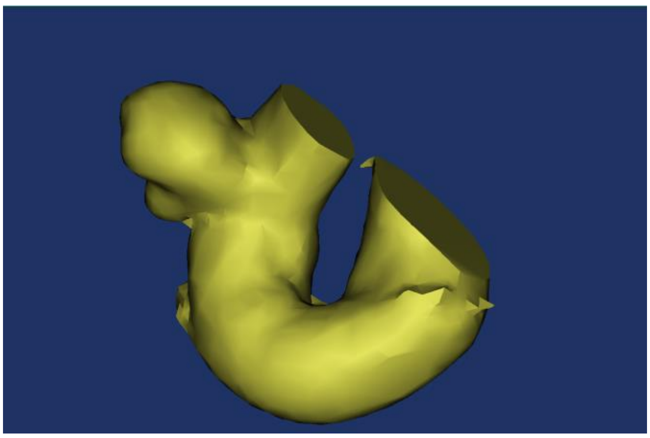

Fig. 1 Segmentation using Mimics Research 19.0.

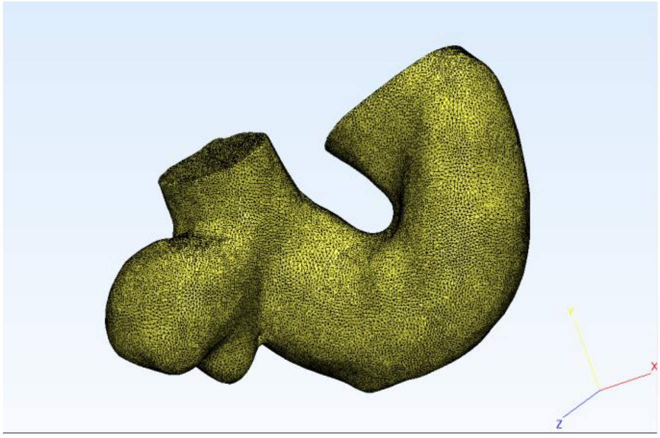

Fig. 2 Mesh Creation using 3-matic Research 11.0

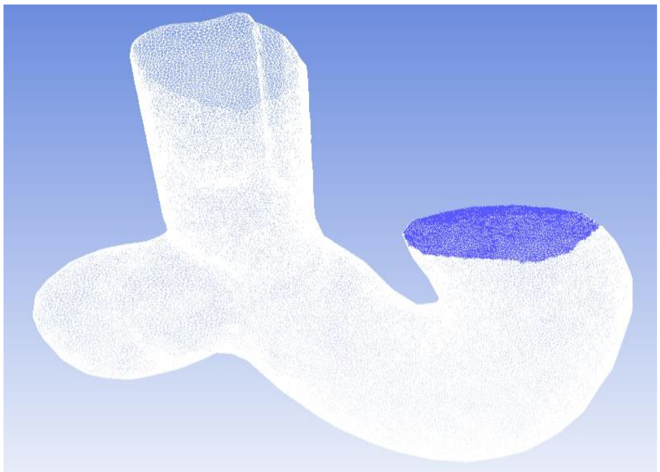

Fig. 3 Final Mesh in ANSYS Fluent 16.0.

Simulation Modeling

ANSYS Fluent 16.0 was used to model the blood flow in the cerebral artery and aneurysm. The mesh file was imported to ANSYS Fluent and checked to ensure the mesh quality. The scaling of the mesh was adjusted to millimeters to correspond to the actual size of the artery. In addition, multiple viewing planes must be created in order to analyze the velocity of blood flow at specific points of the cerebral artery. For this simulation, there were five viewing planes: after the inlet (A), before the aneurysm (B), after the aneurysm (C), before the outlet (D), and a plane parallel to the outlet (E) at the aneurysm. Figure 4 depicts the final mesh that was used for the simulation and Figure 5 shows the location of the view planes; Plane A, Plane B, Plane C, Plane D, Plane E, inlet and outlet.

The simulation solver was specified to Transient Time, of the Pressure-based type, and with Absolute Velocity Formulation. The Discrete Phase Model (DPM) was used to simulate blood cells moving through the cerebral artery. The model was verified from first principles according to the work by Yunus et. al [Ref]' Inert particles with a diameter of 0.02mm and a non-spherical physical model of 1.5 represented the blood cells. The injection of the blood cells was set to the surface type and injected from the inlet of the cerebral artery. In addition to the default DPM settings, "Interaction with Continuous Phase" and "Update DPM Sources Every Flow Iteration" were also checked off under the "Interaction" heading. Under "Contour Plots for DPM variables," the options for "Mean Values" and "RMS Values" were checked. Under the "Tracking" tab, the option "Specify Length Scale" was turned on and the length scale was specified to be 0.1mm.As for the materials needed in the simulation, the fluid was specified as blood. Table 1 shows the parameter conditions for blood. In addition, the inert particle was modified to be blood cells with a density of 1019 kg/m^3.

Table 1 Parameters for blood as a fluid material.

Density (kg/m^3)	Consistency Index (kg-s^n2/m)	Power Law Index (n)	Minimum Viscosity Limit (kg/m-s)	Maximum Viscosity Limit (kg/m-s)	Reference Temperature (K)
1080	0.2073	0.4851	0.00125	0.03	310

Table 2 Reference values for simulation.

Area (m^2)	Density (kg/m^3)	Length (mm)	Temperature (K)	Velocity (m/s)	Viscosity (kg/m-s)	Ratio of Specific Heats
1	1080	1000	288.16	0.3162831	1.7894e-0.5	1.4

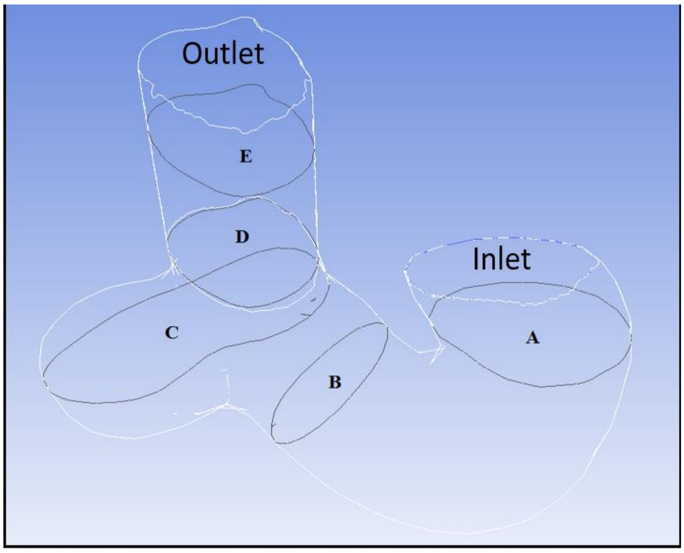

Fig. 4 Location of the five viewing planes.

For the boundary conditions, the inlet of the middle cerebral artery was specified as a velocity inlet with a constant velocity of 0.31m/s taken from the lowest inflow velocity of the pulse that shown in Fig. 6. The inlet flow is the average of velocity in middle cerebral artery of 355 patients. The inlet velocity was represented as "Magnitude, normal to Boundary" method with an absolute reference frame and no initial gauge pressure.. For the outlet of the cerebral artery, it was specified to be a pressure outlet with a gauge pressure of 13332 pascal (99.998mmHg) and the average pressure specification checked. The backflow direction specification method was set to "Normal to Boundary." The DPM setting for the outlet was set to escape.

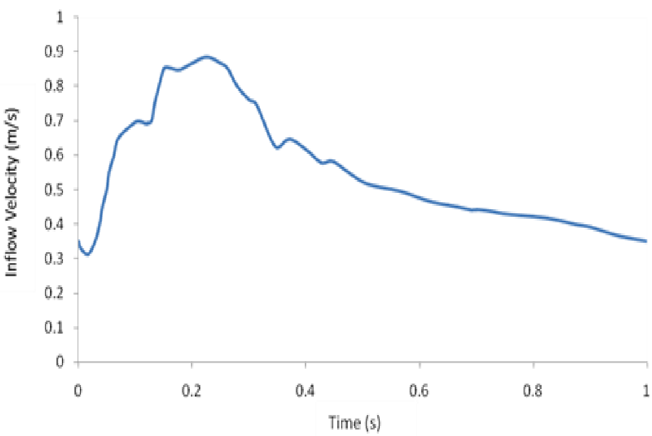

Fig. 6 Inflow velocity profile with the time.

Table 2 shows the values that were inputted for the "Reference Values" task page. Tables 3, 4, and 5 provide the values used for each task page of ANSYS Fluent. For "Monitors" and "Calculation Activities" task pages, none of the options were changed and were left at the default setting. The simulation was run for a total time period of two seconds which takes minimum ten days simulation.

Table 3 Solution controls values.

Pressure	Density	Body Forces	Momentum	Discrete Phase Sources
0.3	1	0.1	0.5	1

Table 4 Solution initialization values.

Gauge Pressure (pascal)	X Velocity (m/s)	Y Velocity (m/s)	Z Velocity (m/s)
0	0.01434163	-0.003352355	0.31594

Table 5 Run calculation values.

Time Step Size (s)	Number of Time Steps	Max Iterations/ Time Step	Reporting Interval	Profile Update Interval
0.0005	4000	300	1	1

In order to analyze the results, the velocity vectors, velocity pathlines, and the wall shear stress were then displayed. The velocity vectors were specified to originate from the viewing planes that were initially created when the mesh was imported. The pathlines were used to validate the movement of the particles and to see the specific trajectory of the particles as they move through the cerebral artery. The wall shear stress was used to determine which locations in the artery experience the highest amount of stress.

RESULTS AND DISCUSSION

The velocity pathlines of the blood cells are shown in Figure 7, where the fastest cells are indicated by red areas while the slowest cells are shown in blue. The spectrum of velocities are shown on the left in units of meters per second (m/s). The fastest blood cells are near the outlet (the long side) and towards the center of the cerebral artery.

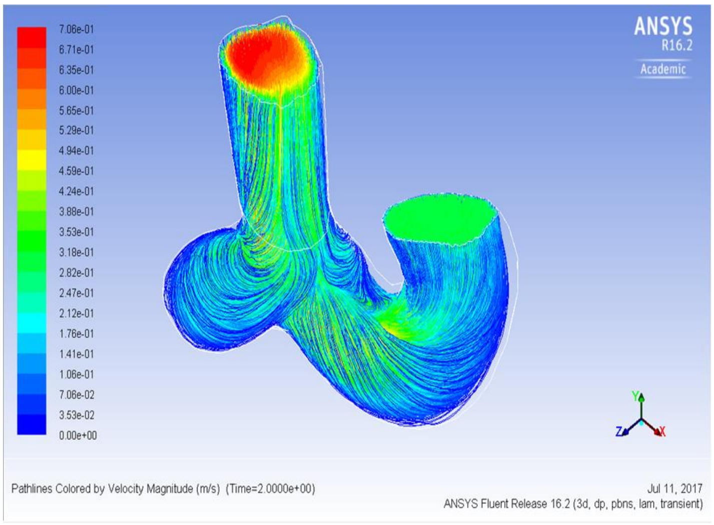

Fig. 7 Velocity pathlines of blood cells.

The Pulse function was used to create an animation of the velocity pathlines as the blood cells traveled through the cerebral artery. The primary interest of this function is to understand how blood flows through the aneurysm. Figure 8a-8b illustrates how the blood flow divided into two streams as it passes through the aneurysm. The main blood flow stream proceeded to the outlet at a faster velocity than the other stream which circulated the aneurysm, as shown in Figure 8c. Eventually, all of the remaining blood cells in the aneurysm flowed towards the outlet shown in Figure 8d.

Velocity vectors were also analyzed at desirable locations, or planes, as mentioned in the Methodology section. Areas with the fastest particles were indicated by red and long arrows. Figure 8a demonstrates that the blood cells generally begin at low velocities. They begin to increase velocities after the first curve of the artery

However, the fastest blood cells were concentrated along the wall of the artery that was opposite of the aneurysm. Figure 8a demonstrates this observation, where the slower blood cells circulated in the aneurysm, or the top half of the artery. The blood cells that did not enter the aneurysm dramatically increased in velocity due to the sharp division between the aneurysm and artery (Figure b). Figures 8 and 9 confirms that the change in velocities is consistent from the sharp division to the outlet.

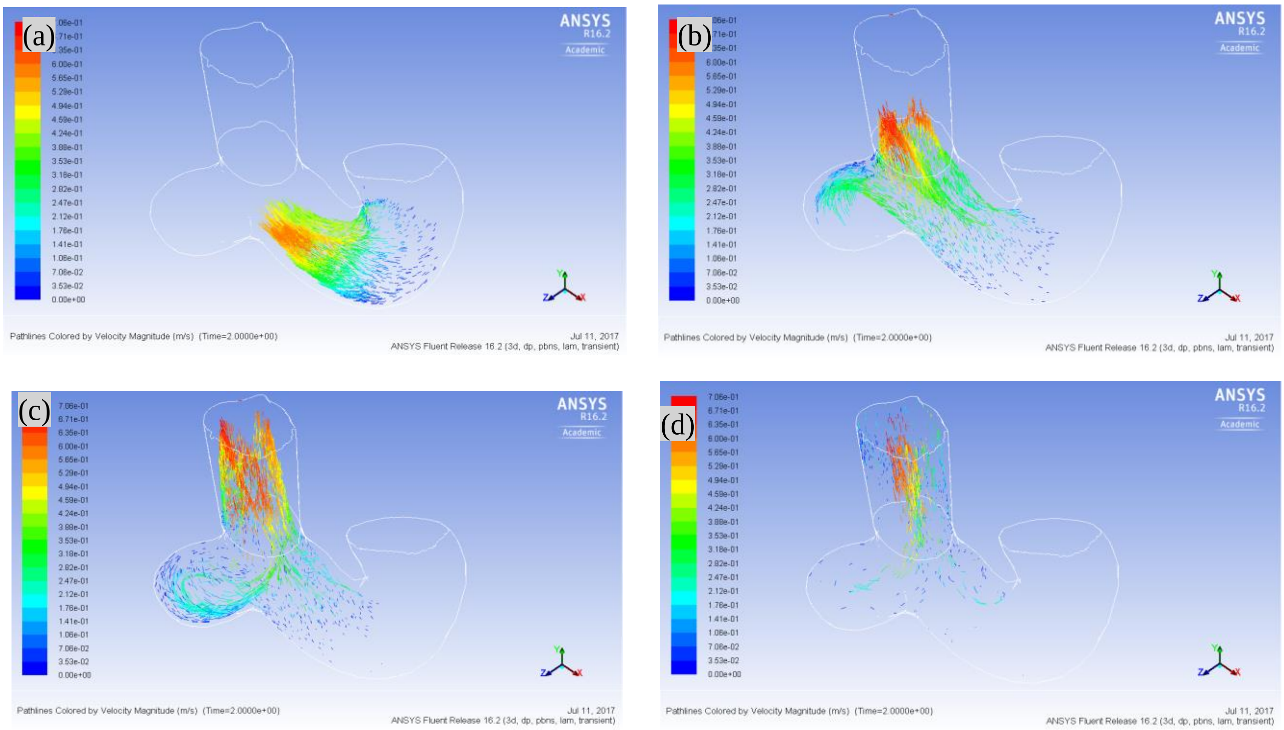

Fig. 8 Velocity pathlines at the aneurysm using the Pulse function. 7a shows a uniform blood flow before reaching the aneurysm. 7b illustrates the division of the blood flow upon reaching the aneurysm 7c displays the circulation of the blood cells remaining in the aneurysm.The remaining blood cells eventually leave the aneurysm, shown in 7d.

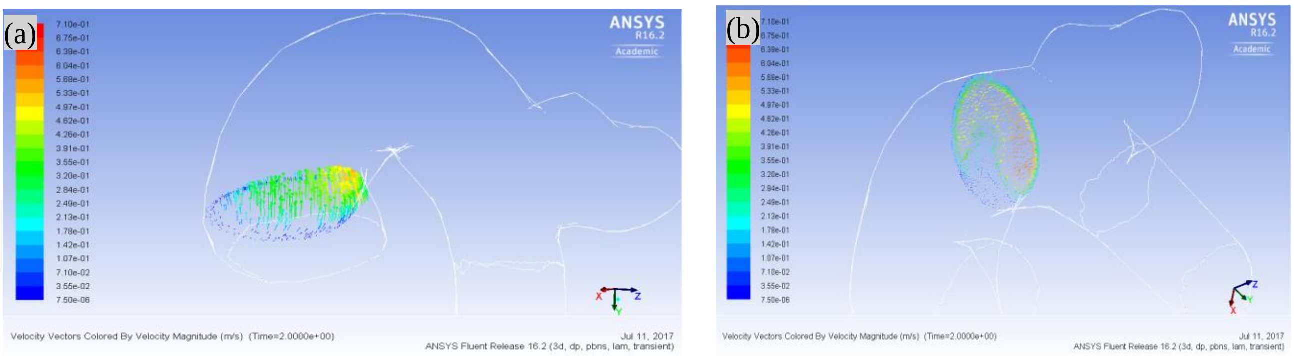

Fig. 9 (a) Velocity Vectors Immediately After Inlet (b) Velocity vectors immediately before the aneurysm.

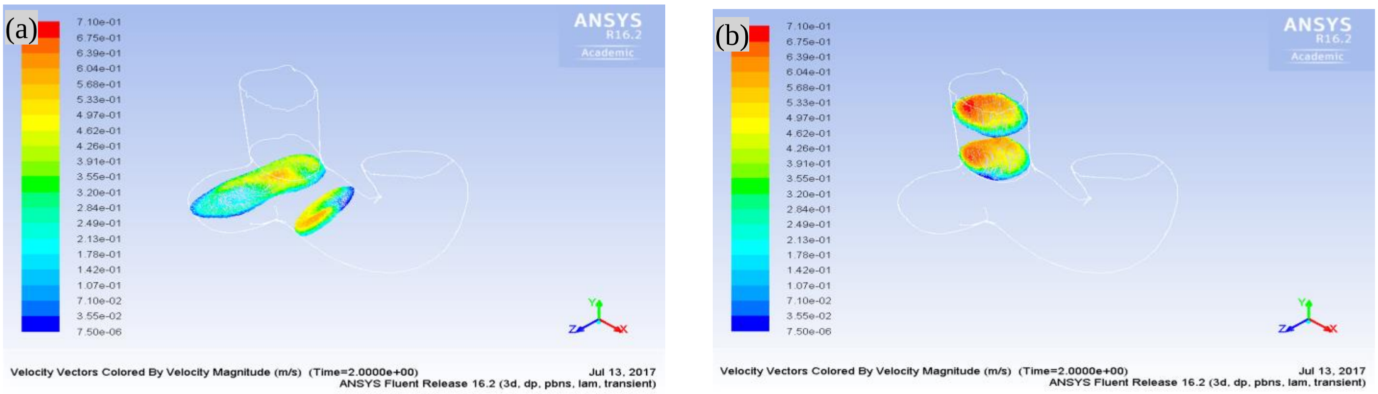

Fig. 10 (a) Velocity Vectors at plane B and plane C (b) Velocity Vectors at plane D and plane E.

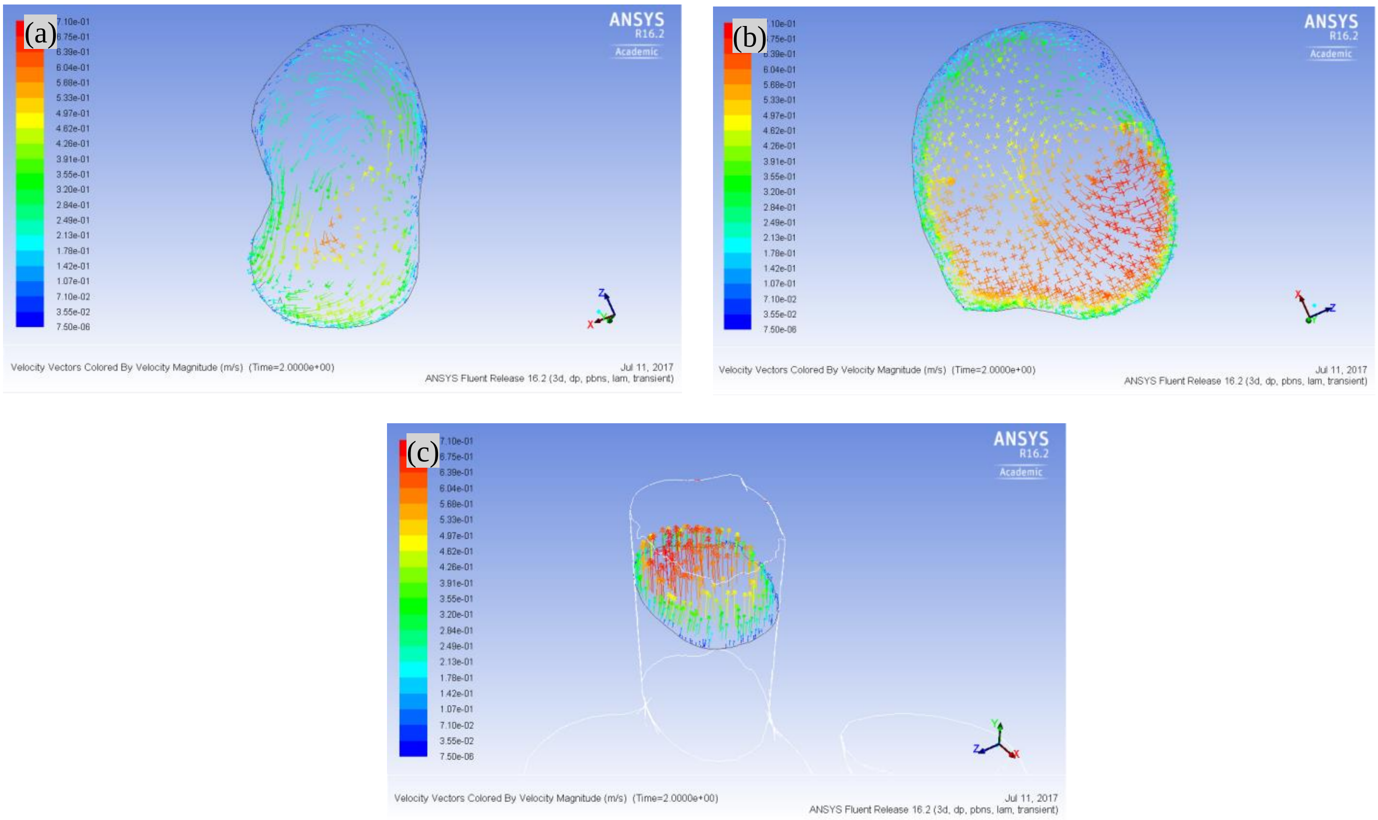

Fig. 11 (a) Plane of aneurysm displaying velocity vectors (b) Plane immediately after aneurysm displaying velocity vectors (c) Velocity vectors immediately before the outlet.

ANALYSIS AND DISCUSSION

In this simulation, Non-Newtonian Power Law model was used to describe the behaviour of blood. When heart is pumping the blood to the vascular network, the artery wall is subjected to of haemodynamic forces. The perpendicular forces resulting from the pressure pulse is responsible for arterial wall distension. The tangential stress exerted by the blood flow is the frictional force known as wall shear stress (WSS). In order to calculate the WSS, the following relationship is used [8]:

$$\tau_w = -\mu\gamma = -\mu\frac{\partial v}{\partial r}$$

where:
τ_w is wall shear stress
μ is viscosity of blood
γ is shear rate

The shear rate, $\dot{\gamma}$ is defined as the radial derivative of blood flow velocity ($\partial v/\partial r$). The WSS is evaluated using the velocity gradient at the wall and almost synonymous with shear rate. High shear rate present when the diameter is small and flow is fast and the low shear rate present when the diameter is large and flow is slow.

WSS is a frictional force between blood and endothelium of the artery. At any point where a high velocity was observed, the WSS intensified. However, the greatest stress occur at the neck of aneurysm. This observation agrees the WSS equation $\tau w = -\mu\gamma = -\mu(\partial v/\partial r)$. The leave the region due to high flow velocity. At the region where the velocity is slow, the WSS is conversely reduced.

Consequently, some of the cells will not have enough momentum to leave the aneurysm area quickly. It was noted that the thinning of artery wall depended on the interaction between platelets, blood cells

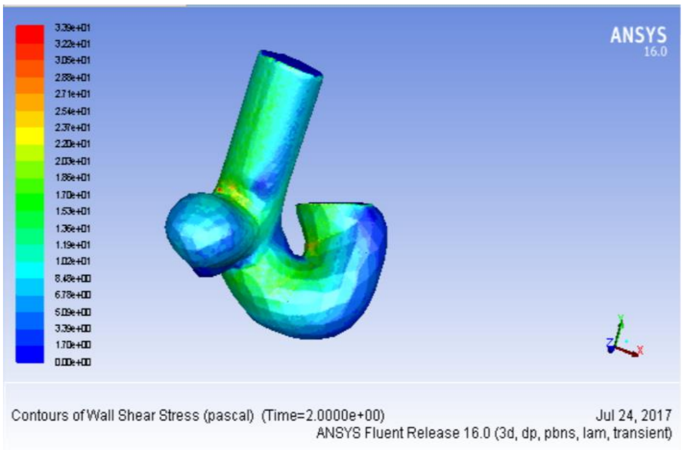

Fig. 11 Wall shear stress distribution.

and smooth muscle cells (Cebral, Castro, Burgess, et al., 2005). Hence, the risk of rupture could increase as indicated in the velocity field, where the highest velocity is at the neck of the aneurysm where the blood cells are entering and leaving the aneurysm dome. There is a significant change in the flow cross-sectional area. Sudden change in velocity may cause the abrupt pressure loss in aneurysm area. The velocity reduced and the flow recirculation formed at low pulse rate.

In this study, WSS distribution was determined considering the presence of blood cells. These blood cells will transport according to the velocity of the blood and it will trapped or remained at that area. As in Fig 11, the highest wall shear stress was at the neck of the aneurysm where there is a changing of velocity. In the end it will cause the tissue to the tear and caused aneurysm ruptured. For this study the lowest ranges is from 0.00 to 3.39 Pascal where the highest WSS will be at the neck of the aneurysm. Hence, the risk of rupture could increase at the highest velocity where the blood cells are entering and leaving the aneurysm dome because there is a significant change in the flow cross-sectional area and sudden change in velocity may cause the abrupt pressure loss in aneurysm area. High blood cells concentration was found located at the aneurysm dome where the flow is very low. The blood cell residence time also reported to be high and a lot of blood cell were accumulated at the dome before leaving the aneurysm region. The WSS at the aneurysm dome is low because velocity inlet is slow or nearly stagnant.

FUTURE WORK

Despite the noticeable correlation between WSS and blood cell velocities, this is merely one aneurysm case. Every patient's aneurysm has a unique shape and position along the artery. Both of these characteristics ultimately contribute to varying blood cell velocities and different risks of rupture. More patient studies may yield different correlations between WSS and blood cell velocities. Another critical factor in determining rupture is WSS. While WSS values are obtainable through current results, the exact value of rupture is still undetermined since it varies with each patient. Once a range of WSS values are established through additional patient studies, it can be compared with literature values for maximum WSS of a cerebral artery**.**

ACKNOWLEDGEMENT

This research is funded by Ministry of Science, Technology and Innovation (MOSTI) under Project No: 06-02-02-SF0194. The authors are also thankful to HPC3 Universiti Teknologi PETRONAS for their facilities, support and help.

REFERENCES

Can, A., Du, R. 2016. Association of hemodynamic factors with intracranial aneurysm formation and rupture, *Neurosurgery*, *78*(4), 510-520.

Cebral, J., Castro, M., Appanaboyina, S., Putman, C., Millan, D., Frangi, A. 2005. Efficient pipeline for image-based patient-specific analysis of cerebral aneurysm hemodynamics: Technique and sensitivity. *IEEE Transactions on Medical Imaging*, *24*(4), 457-467.

Cebral, J. R., Castro, M. A., Appanaboyina, S., Putman, C. M., Millan, D., Frangi, A. F. 2005. [62]Efficient pipeline for image-based patient-specific analysis of cerebral aneurysm hemodynamies technique and sensitivity. *IEEE Transactions on Medical Imaging*, *24*(4), 457–467.

Cebral, J. R., Castro, M. a., Burgess, J. E., Pergolizzi, R. S., Sheridan, M. J., Putman, C. M. (2005). Characterization of cerebral aneurysms for assessing risk of rupture by using patient-specific computational hemodynamics models. *American Journal of Neuroradiology*, *26*(10), 2550–2559.

Dhar, S., Tremmel, M., Mocco, J., Kim, M., Yamamoto, J., Siddiqui, A., Hopkins, L., Meng, H. 2008. Morphology parameters for intracranial aneurysm rupture risk assessment. *Neurosurgery*, *63*(2), 185-197.

Goubergrits, L., Schaller, J., Kertzscher, U., van den Bruck, N., Poethkow, K., Petz, C., Hege, H., Spuler, A. 2011. Statistical wall shear stress maps of ruptured and unruptured middle cerebral artery aneurysms. *Journal of the Royal Society Interface*, *9*(69), 677-688.

Goubergrits, L., Schaller, J., Kertzscher, U., van den Bruck, N., Poethkow, K., Petz, C., … Spuler, A. (2012). Statistical wall shear stress maps of ruptured and unruptured middle cerebral artery aneurysms. *Journal of The Royal Society Interface*, *9*(69), 677–688.

Jiang, Y., Lan, Q., Wang, Q., Lu, H., Ge, F., Wang, Y. 2014. Correlation between the rupture risk and 3D geometric parameters of saccular intracranial aneurysms. *Cell Biochemistry and Biophysics*, *70*(2), 1417-1420.

Munarriz, P. M., Gómez, P. A., Paredes, I., Castaño-Leon, A. M., Cepeda, S., Lagares, A. (2016). Basic Principles of Hemodynamics and Cerebral Aneurysms. *World Neurosurgery*, *88*, 311–319.

Munarriz, P. M., Gómez, P. A., Paredes, I., Castaño-Leon, A. M., Cepeda, S. Lagares, A. 2016. Basic principles of hemodynamics and cerebral aneurysms. *World Neurosurgery*, *88*, 311-319.

Nur, H., Hayati, F., Hamdan, H. 2007. On the location of different titanium sites in Ti-OMS-2 and their catalytic role in oxidation of styrene. *Catalysis Communications*, *8*, 2007-2011.

Nur, H., Guan, L. C., Endud, S., Hamdan, H. 2004. Quantitative measurement of a mixture of mesophases cubic MCM-48 and hexagonal MCM-41 by ^{13}C CP/MAS NMR. *Materials Letters, 58*(12-13), 1971-1974.

Papaioannou, T. G., Stefanadis, C. (2005). Vascular wall shear stress: basic principles and methods. *Hellenic Journal of Cardiology*, *46*(1), 9–15.

Xiang, J., Natarajan, S., Tremmel, M., Ma, D., Mocco, J., Hopkins, L., Siddiqui, A., Levy, E., Meng, H. 2010. Hemodynamic-morphologic discriminants for intracranial aneurysm rupture. *Stroke*, *42*(1), 144-152.

Xiang, J., Natarajan, S. K., Tremmel, M., Ma, D., Mocco, J., Hopkins, L. N., … Meng, H. (2011). Hemodynamic-morphologic discriminants for intracranial aneurysm rupture. *Stroke*, *42*(1), 144–152.